Journal of Statistical Mechanics:
Theory and Experiment

PAPER: INTERDISCIPLINARY STATISTICAL MECHANICS

Optimal weighted coefficient for heterogeneous epidemic spreading networks

Journal of Statistical Mechanics: Theory and Experiment
An IOP and SISSA journal

PAPER: Interdisciplinary statistical mechanics

Optimal weighted coefficient for heterogeneous epidemic spreading networks

Xuming An[1], Li Ding[1], Ping Hu[1] and Yi Yu[2]

[1] School of Electrical Engineering and Automation, Wuhan University, Wuhan 430072, People's Republic of China
[2] School of Automation Engineering, University of Electronic Science and Technology of China, Chengdu 610054, People's Republic of China
E-mail: liding@whu.edu.cn

Received 16 June 2018
Accepted for publication 19 October 2018
Published 13 December 2018

Online at stacks.iop.org/JSTAT/2018/123402
https://doi.org/10.1088/1742-5468/aaeb45

Abstract. In this paper, we study epidemic spreading on an arbitrary heterogeneous undirected weighted network, in which reinforcement effects among pathogens are considered to depict the characteristics of multiple infection based on a novel propagation model. In order to characterize the formation mechanism of contact weight between individuals, a new parameter defined as the weighted coefficient is introduced to coordinate each individual's own expected weights towards neighbors. A reasonable candidate for the expected weight relating to individual sensitivity and neighbor's infection level is also provided. Furthermore, an optimization problem is formulated to address a trade-off between individuals' infection levels and the adjustment of their weighted coefficients. The existence of an optimal solution is analyzed and the general expression of an optimal weighted coefficient is obtained. Numerical simulations performed by adopting the forward–backward sweep method are presented to illustrate the validity and efficiency of our theoretical results.

Keywords: epidemic modelling, network dynamics, optimization over networks, random graphs, networks

1742-5468/18/123402+23$33.00

Contents

1. Introduction

Spreading processes are ubiquitous in nature, occurring wherever there exist contact or communication possibilities, ranging from epidemic or malware spreading [1–4], rumor or information dissemination [5–7] to power grid cascading failures [8–10]. Exploring the characteristics of a dynamical spreading process is essential for diverse disciplines of applied mathematics, sociology, physics and cybernetics [11–14]. In recent decades, the study of epidemic spreading over complex networks has attracted intense attention. A large number of relevant works have been rapidly carried out, employing compartment models such as the susceptible-infected-susceptible (SIS), susceptible-infected-recovered (SIR) models and other derived models [15–18].

Most of these works have been studied under a framework where only one single pathogen is considered in the network, which is far removed from the practical case where multiple pathogens are involved in the spreading process simultaneously. Recently, the modeling and analyzing of the spreading process with multiple pathogens have become hot topics in this area, and diverse relationships among pathogens have been considered. For instance, the relationship among pathogens can be competitive [19–22], in which the propagation abilities of pathogens are mutually inhibited and each individual can only be occupied by the dominant pathogen at each time. Watkins *et al* [19] considered a competitive epidemic process on a bilayer network and developed a framework to find an optimal allocation of control resources for eliminating one of the epidemics. Darabi Sahneh *et al* [21] proposed the SI_1I_2S model of two

J. Stat. Mech. (2018) 123402

exclusive, competitive viruses over a two-layer network and introduced the concepts of survival threshold and absolute-dominance threshold. In contrast, the relationship among pathogens can also be cooperative [23–27], in which the infection rate of one pathogen may be enhanced by the spreading of other pathogens. A representative example is that when an individual is infected with a pathogen their immunity will reduce, resulting in an increased possibility of being infected by another pathogen. Cui *et al* [25] considered the SIR model with two mutually cooperative pathogens. Their work clarified the effect of heterogeneity and system size on the nature of the transition and validated the physical interpretation about the origin of discontinuity. Besides, there are also several works involving both competitive and cooperative relationships among pathogens, such as [28]. In addition to the above cases, another case of multiple infection is common but rarely considered, where the spreading of pathogens has no significant effect on each other, however, their coexistence in individuals may lead to a reinforcement effect, which can be fatal. Therefore, such a phenomenon in multiple infection deserves to be studied.

Since the outbreak of epidemics may lead to widespread panic and economic loss in human society, an intervention strategy to suppress epidemics is necessary. In recent years, researchers have devoted themselves to the development of various suppression methods. From the control point of view, the spreading process can be regarded as a dynamical system, and different intervention strategies can be applied with respect to diverse control variables [29–37]. In previous literature, a novel idea has been to adjust the contact weights between individuals. Through strategies such as heuristic control and optimal control, contact weights are controlled to change connection or communication strength between individuals, thereby reducing the probability of infection. It has been proved that the control of contact weights can achieve better performance and reflect the dynamical evolution trend of individual behavior in the spreading process. Feng *et al* [31] presented a heuristic weight control strategy according to the global and local infective information spreading. Hu *et al* [34] studied the individual-based optimal weight adaption for a heterogeneous epidemic spreading network under the trade-off function. For an undirected weighted network, the edge between two individuals has no directional properties and its contact weight can be determined by a third party's assignment or negotiation between individuals, which always regard the willingness of both parties as reference. For instance, in research collaboration networks, contact weight is expressed in terms of collaborative papers or projects between scientific researchers. It is natural that before establishing the cooperation formally, a scientific researcher may form the initial will to cooperate according to several factors, such as subject relevance, scientific research capabilities, environment and facilities, time schedules, etc. In a social network, contact weight is equivalent to meeting frequency between individuals. Before the meeting frequency is determined, two friends routinely express their own willingness to meet based on several factors, such as degree of closeness, purpose of meeting, distance, etc. However, the majority of previous works have few considerations of this aspect. Thus, in this paper, we define the individual's contact willingness as *expected weight* and introduce a new parameter called *weighted coefficient* as the result of assignment or negotiation to coordinate the proportion of two parties' expected weights, which constructs the mechanism of contact weight formation. Furthermore, for the previous optimal control problem of contact weight similar to

J. Stat. Mech. (2018) 123402

[34], contact weight is no longer the optimization variable, once we consider its formation mechanism. Naturally, the relevant factor involving formation will be chosen as the optimization variable and the weighted coefficient plays exactly such a role in this paper. These studies are able to achieve the desired goals and reveal the evolution of individual behavior, which may be beneficial for understanding the epidemic spreading process more comprehensively.

Based on the above considerations, the main contents in this paper can be described as follows. Firstly, we propose a novel epidemic spreading model to depict the reinforcement effect on multiple infection by observing that multiple infected individuals may have negligible recovery rate compared to single infection. Secondly, a new parameter called the weighted coefficient is introduced to determine the contact weight between individuals combined with their own expected weights towards neighbors. Then an optimal problem is constructed, in which the weighted coefficient is regarded as the optimization variable to minimize the possible aggregated cost of epidemic spreading and weighted coefficient adjustment. Thirdly, we prove the existence of solutions to the proposed problem and obtain the general structure of the optimal solution. Finally, numerical simulations employing the forward–backward sweep method are conducted on networks with different topology to verify our theoretical results.

The rest of this paper is organized as follows. In section 2, the dynamics of epidemic spreading with multiple infection is described by mean-field approximation and its bahavior analysis. Meanwhile, the formation mechanism of contact weight based on weighted coefficient is provided. In section 3, the optimal control problem of the weighted coefficient is studied. The existence and structure of an optimal solution are provided. Numerical simulations are performed to illustrate theoretical results in section 4. Conclusions are drawn in section 5.

2. Preliminaries and problem definition

2.1. Graph theory

A weighted, undirected graph is defined as the triad $\mathcal{G} \triangleq (\mathcal{V}, \mathcal{E}, \mathcal{W})$ with a finite set of nodes $\mathcal{V} = \{1, 2, ..., N\}$ and edges set $\mathcal{E} \subseteq \mathcal{V} \times \mathcal{V}$. An edge between node i and j means they can exchange information and influence the update of state mutually in the spreading process. $\mathcal{W} = [w_{ij}] \in R^{N\times N}$ is the weighted adjacency matrix of the network, where element $\omega_{ij} \in [0, 1]$ is the contact weight related to the edge between node i and j. $\omega_{ij} > 0$ if $(i, j) \in \mathcal{E}$ and $\omega_{ij} = 0$ otherwise. Due to the symmetry of the weighted adjacency matrix, $\omega_{ij} = \omega_{ji}, i, j \in \mathcal{V}$. In a dynamic network in which the contact weight is time-varying, the original weighted adjacency matrix is denoted by $\mathcal{W}^o = [w^o_{ij}]$. Accordingly, contact weight is always constant in a static network.

2.2. Weighted SI_1I_2RL-based network model formulation

We consider two pathogens with different pathogenicity spreading on the network. A compartment model SI_1I_2RL is adopted, which classifies the whole population into

J. Stat. Mech. (2018) 123402

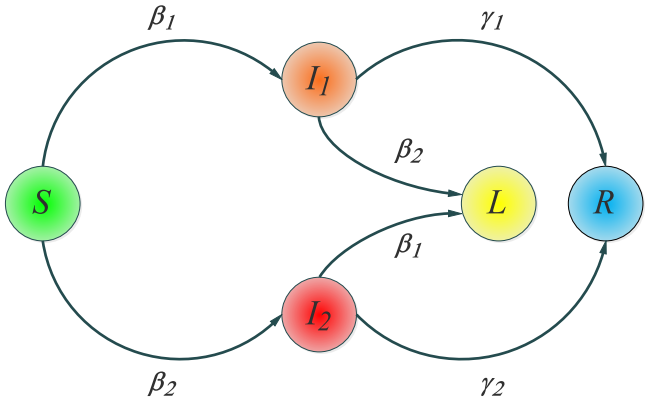

Figure 1. The status transition diagram of the SI_1I_2RL model.

five groups: *Susceptible* (S), $Infected$ (I_1 and I_2), *Recovered* (R) and *Limited* (L). *Susceptible* is a group of individuals who are not infected by any pathogen. $Infected$ contains the individuals infected by pathogen 1 or 2 respectively and *Recovered* is a group of recovered individuals. *Limited* individuals are those infected by both pathogens simultaneously. It is assumed that the recovery rate of individuals in group L is absent because of multiple infection. Besides, due to the limited contact of individuals with multiple infection, such as death or isolation, we do not consider their infectivity.

The state transitions are shown in figure 1. A susceptible individual would become infectious with constant infection rate $\beta_1 > 0$ ($\beta_2 > 0$) if they come into contact with individuals infected by pathogen 1 (2). Similarly, an individual infected with pathogen 1 (2) may be infected and transform into a limited state with infection rate $\beta_2 > 0$ ($\beta_1 > 0$) when coming into contact with other individuals infected by pathogen 2 (1). Individuals infected with pathogen 1 (2) may recover with recovery rate $\gamma_1 > 0$ ($\gamma_2 > 0$).

A connected, undirected and heterogeneous network consisting of N individuals is considered in this paper. Denote $p_i^S(t), p_i^{I_1}(t), p_i^{I_2}(t), p_i^L(t), p_i^R(t) \in [0,1]$ as the probability of individual i being susceptible, infected by pathogen 1, infected by pathogen 2, limited and recovered at time t, respectively. Obviously, we have the normalization condition

$$p_i^S(t) + p_i^{I_1}(t) + p_i^{I_2}(t) + p_i^L(t) + p_i^R(t) \equiv 1, t \geqslant 0, i = 1, 2, ..., N. \tag{2.1}$$

If the number of individuals is sufficient, the average of all the individuals' probabilities in each state can be equivalent to the density of individuals in the corresponding state.

The discrete-time mathematical model based on the microscopic Markov chain approach is proposed as

$$\begin{cases} p_i^S(t+1) = (1 - q_i^{SI_1}(t) - q_i^{SI_2}(t))\, p_i^S(t), \\ p_i^{I_1}(t+1) = p_i^{I_1}(t) + q_i^{SI_1}(t)\, p_i^S(t) - \gamma_1 p_i^{I_1}(t) - q_i^{I_1L}(t)\, p_i^{I_1}(t), \\ p_i^{I_2}(t+1) = p_i^{I_2}(t) + q_i^{SI_2}(t)\, p_i^S(t) - \gamma_2 p_i^{I_2}(t) - q_i^{I_2L}(t)\, p_i^{I_2}(t), \\ p_i^L(t+1) = p_i^L(t) + q_i^{I_1L}(t)\, p_i^{I_1}(t) + q_i^{I_2L}(t)\, p_i^{I_2}(t), \end{cases} \tag{2.2}$$

for $i = 1, 2, ..., N$, where

$$\begin{cases} q_i^{SI_1}(t) = q_i^{I_2L}(t) = 1 - \prod\limits_{j\in N_i}(1-\beta_1 p_j^{I_1}(t)\omega_{ij}(t)), \\ q_i^{SI_2}(t) = q_i^{I_1L}(t) = 1 - \prod\limits_{j\in N_i}(1-\beta_2 p_j^{I_2}(t)\omega_{ij}(t)), \end{cases} \tag{2.3}$$

$q_i^{SI_1}(t)$ and $q_i^{SI_2}(t)$ represent the probability that susceptible individual i is infected by the adjacent individuals infected by pathogen 1 or 2, respectively; $q_i^{I_1L}(t)$ denotes the probability that individual i infected with pathogen 1 is infected and transformed into the limited state after coming into contact with all their neighbors; the similar definition holds for $q_i^{I_2L}(t)$.

Under two assumptions that the states of one's neighbors should be independent of each other [38–40] and the infection rates β_1 and β_2 are small enough, we can derive

$$\begin{cases} q_i^{SI_1}(t) = q_i^{I_2L}(t) \approx \sum\limits_{j=1}^{N}\beta_1 p_j^{I_1}(t)\omega_{ij}(t), \\ q_i^{SI_2}(t) = q_i^{I_1L}(t) \approx \sum\limits_{j=1}^{N}\beta_2 p_j^{I_2}(t)\omega_{ij}(t). \end{cases} \tag{2.4}$$

Then, the mean-field model can be written as

$$\begin{cases} \dot{p}_i^S(t) = (-\sum\limits_{j=1}^{N}\beta_1 p_j^{I_1}(t)\omega_{ij}(t) - \sum\limits_{j=1}^{N}\beta_2 p_j^{I_2}(t)\omega_{ij}(t))\, p_i^S(t), \\ \dot{p}_i^{I_1}(t) = \sum\limits_{j=1}^{N}\beta_1 p_j^{I_1}(t)\omega_{ij}(t)\, p_i^S(t) - \gamma_1 p_i^{I_1}(t) - \sum\limits_{j=1}^{N}\beta_2 p_j^{I_2}(t)\omega_{ij}(t) p_i^{I_1}(t), \\ \dot{p}_i^{I_2}(t) = \sum\limits_{j=1}^{N}\beta_2 p_j^{I_2}(t)\omega_{ij}(t)\, p_i^S(t) - \gamma_2 p_i^{I_2}(t) - \sum\limits_{j=1}^{N}\beta_1 p_j^{I_1}(t)\omega_{ij}(t) p_i^{I_2}(t), \\ \dot{p}_i^{L}(t) = \sum\limits_{j=1}^{N}\beta_2 p_j^{I_2}(t)\omega_{ij}(t)\, p_i^{I_1}(t) + \sum\limits_{j=1}^{N}\beta_1 p_j^{I_1}(t)\omega_{ij}(t) p_i^{I_2}(t), \end{cases} \tag{2.5}$$

for $i = 1, 2, ..., N$.

2.3. Model behavior analysis

There are two possible scenarios when the system (2.5) reaches steady-state, that is, the coexistence of three remaining states S, L, R or two remaining states L, R, which are determined by the spreading parameters as infection rates and recovery rates.

In order to grasp the characteristics of system (2.5), assume contact weights are static constants. Without loss of generality, set $\omega_{ij} = 1, i, j = 1, 2, ..., N$. Then we provide three phase diagrams as shown in figure 2, which illustrate the relationship between two pathogens' transmission ratios (i.e. the ratio of infection rate to recovery rate, β_1/γ_1 and β_2/γ_2) and the density of individuals in each state at the steady-state stage. Transition ratio may vary with different values of infection rate β_1, β_2 and recovery rates γ_1, γ_2. As can be seen intuitively, there exists the process with continuous phase transition. From figure 2(a), it can be concluded that individuals in the susceptible state may survive only if the condition that the two pathogens' transmission ratios are both small is satisfied. An increase in any pathogen's transmission ratio will result in a corresponding decrease in susceptible individuals' density. A small transmission ratio

J. Stat. Mech. (2018) 123402

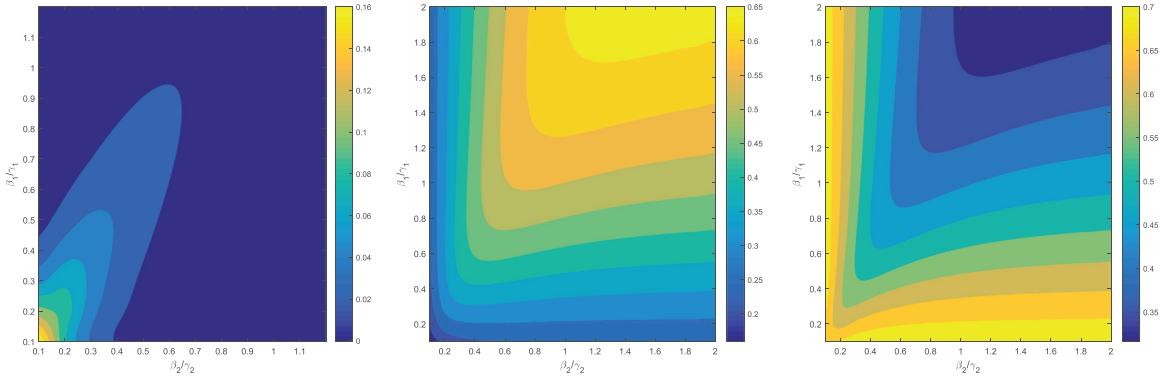

(a) (b) (c)

Figure 2. Phase diagrams of individual densities in different states at the steady-state stage. (a) Individual density in S state. (b) Individual density in L state. (c) Individual density in R state.

means that the probability of a susceptible individual being infected by neighbors is relatively low and the infected individual has a greater propensity to recover naturally, which may result in the absence of infected individuals in the network before all individuals have ever been infected. Note that there are obvious bulges of non-zero zone in figure 2(a). This is because when the infection rates of two pathogens are similar, they will transform into the limited state with greater contact probability, thereby reducing the infection probability of susceptible individuals. As for the steady-state densities of limited and recovered individuals, the results are demonstrated by figures 2(b) and (c). Only one pathogen having a high transmission ratio may not increase the density of limited individuals, since the formation of the limited state depends on the contact of two kinds of infected individuals. Specifically, a smaller transmission ratio of any pathogen restricts the density of infected individuals, thereby affecting the transition probability of the limited state, allowing more individuals to naturally return to the recovered state.

2.4. Contact weight formation mechanism

As mentioned above, contact weights between individuals are associated with individuals' expected weights towards their neighbors, and a new parameter called the *weighted coefficient* is introduced to control the adopted proportion of expected weights. Thus, there is a mathematical expression given as

$$\omega_{ij}(t) = \mu_{ij}(t)x_{ij}(t) + \mu_{ji}(t)x_{ji}(t), \tag{2.6}$$

where $\mu_{ij}(t) \in [0, 1]$ and $x_{ij}(t) \in [0, 1]$ represent the weighted coefficient and the expected weight from individual i to their neighbor j respectively. The definitions for $\mu_{ji}(t)$ and $x_{ji}(t)$ are similar. Here we assume that $\mu_{ij}(t) + \mu_{ji}(t) = 1$ to maintain $\omega_{ij} \in [0, 1]$.

Furthermore, we consider the expected weight of an individual to be time-varying, always depending on their neighbors' infection level and their sensitivity towards this infection level under given initial conditions, namely

$$x_{ij}(t) = g\left(x_{ij}^0, \psi_{ij}(t), \eta_i\right), \tag{2.7}$$

J. Stat. Mech. (2018) 123402

where $x_{ij}^0 \in [0,1]$ denotes the initial expected weight of individual i to their neighbor j; $\psi_{ij}(t)$ represents the infection level of individual i's neighbor j at time t; η_i is the sensitivity coefficient which is a constant reflecting the individual sensitivity (or aversion tendency) to the epidemic, and the individual sensitivity becomes smaller (larger) as η_i increases (decreases).

Then, we provide a reasonable candidate for $x_{ij}(t)$ as

$$x_{ij}(t) = x_{ij}^0 \theta_{ij}(t), \tag{2.8}$$

where $\theta_{ij}(t) = \frac{1}{1-\mathrm{e}^{-\eta_i}}\left(1-\mathrm{e}^{\psi_{ij}(t)-\eta_i}\right)$ and $\psi_{ij}(t) = p_j^{I_1}(t) + p_j^{I_2}(t), j \in N_i$. θ_{ij} presents the ratio of $x_{ij}(t)$ to x_{ij}^0, reflecting the variation tendency of expected weight compared to initial value over time. What is more, in order to guarantee the non-negativity of $\theta_{ij}(t)$, we limit $\eta_i \geqslant \max\left(p_j^{I_1}(t) + p_j^{I_2}(t)\right), \forall t \geqslant 0$. The schematic diagram of contact weight formation mechanism is shown in figure 3.

Note that θ_{ij} (or x_{ij}) is given as the convex combination. Derivative $\theta_{ij}(t)$ towards η_i, $\frac{\partial\theta_{ij}(t)}{\partial\eta_i} = \frac{\mathrm{e}^{-\eta_i}(\mathrm{e}^{\psi_{ij}(t)}-1)}{(1-\mathrm{e}^{-\eta_i})^2} \geqslant 0$, $\frac{\partial^2\theta_{ij}(t)}{\partial{\eta_i}^2} = -\frac{(\mathrm{e}^{\psi_{ij}(t)}-1)(\mathrm{e}^{\eta_i}-\mathrm{e}^{-\eta_i})}{(\mathrm{e}^{\eta_i}+\mathrm{e}^{-\eta_i}-2)^2} \leqslant 0$, which are not always equal to 0 for $\forall\eta_i > 0$. Thus, $\theta_{ij}(t)$ is a monotonically non-decreasing convex function respective to η_i. That is to say, an individual's expected weight to their neighbors may become larger (smaller) as η_i increases (decreases) with lower (higher) rate of change, which is consistent with the real occasion that when a neighbor's infection level is fixed, an individual's risk awareness may be significantly heightened by the increase in their sensitivity, making the individual more inclined to reduce the expected weight towards the neighbor. Besides, derivative $\theta_{ij}(t)$ towards $\psi_{ij}(t)$, $\frac{\partial\theta_{ij}(t)}{\partial\psi_{ij}(t)} = \frac{\partial^2\theta_{ij}(t)}{\partial\psi_{ij}(t)^2} = -\frac{1}{1-\mathrm{e}^{-\eta_i}}\mathrm{e}^{\psi_{ij}(t)-\eta_i} < 0$. It is proved that $\theta_{ij}(t)$ is a monotonically decreasing convex function respective to $\psi_{ij}(t)$, which means an individual's expected weight to their neighbors may be smaller (larger) as the neighbor's infection level increases (decreases) with higher (lower) rate of change. In other words, the risk awareness of an indvidual with determined sensitivity will be strengthened sharply with the increase of a neighbor's infection, making the individual more inclined to maintain low expected weight towards their neighbor. The relationship between $\theta_{ij}(t), \psi_{ij}(t)$ and η_i is shown in figure 4.

3. Optimal weighted coefficient problem

In this section, a global optimization problem is constructed, in which the optimal weighted coefficients relating to individuals and their neighbors are determined in order to achieve the objective of global optimum. On the one hand, there usually exists an infection cost for individual i with respect to $p_i^{I_1}$, $p_i^{I_2}$, p_i^L. However, since an individual infected by pathogen 1 or 2 can be cured while this is impossible for a limited individual, we only concentrate on the infection cost related to p_i^L, represented as J_1. On the other hand, the adjustment of the individual weighted coefficient may destroy the original balance among the individuals and a certain price needs to be paid, thus it is necessary to consider the cost caused by the variation of weighted coefficient, namely

J. Stat. Mech. (2018) 123402

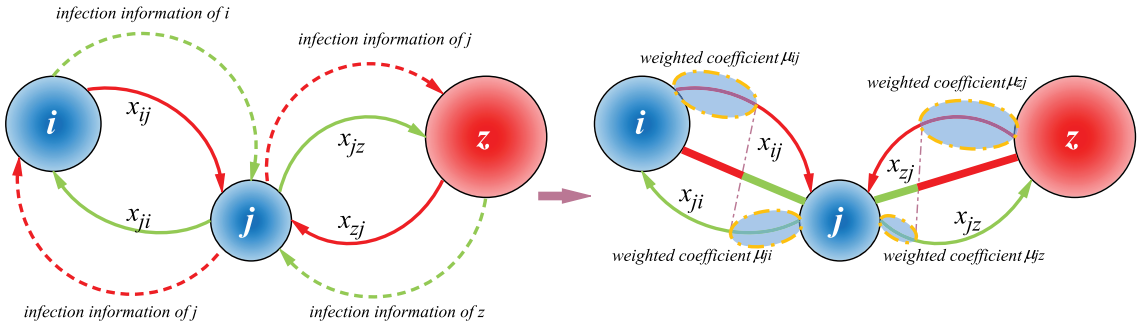

Figure 3. Schematic diagram of contact weight formation mechanism. (In the diagram on the left, the node color indicates the individual state, the dash line denotes feedback information of infection and the solid line indicates an individual's expected weight towards neighbors. The individual receives their neighbor's infection information, and combines their own sensitivity to generate the expected weight towards the neighbor. In the diagram on the right, the shaded portion in dashed box represents the adoption part of an individual's expected weight. The straight solid line indicates the contact weight between individuals and contains two colors indicating that contact weight is determined by the two parties jointly. Weighted coefficient is determined by negotiation or assignment based on individuals' expected weights, thereby forming the contact weight.)

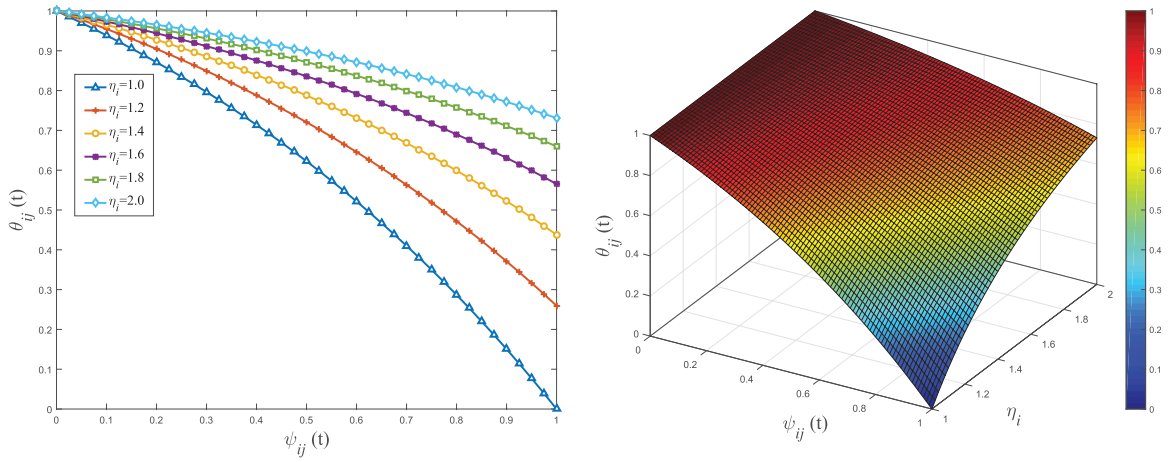

(a) (b)

Figure 4. Relationship between performance indicators of $x_{ij}(t)$. (a) $\theta_{ij}(t)$ versus $\psi_{ij}(t)$ under different η_i. (b) Relationship between $\theta_{ij}(t)$, $\psi_{ij}(t)$ and η_i.

adjustment cost, represented as J_2. Therefore, the objective function is aggregated from these two kinds of costs for all individuals. We consider an accumulative cost throughout the whole time interval, namely total cost, represented as J.

Define Q^C as the Lebesgue square integrable control set of all admissible values of $\mu_{ij}(t)$ over time interval $[0, T]$, given as $Q^C = \{\mu_{ij}(t) \in L^2[0, T] : 0 \leqslant \mu_{ij}(t) \leqslant 1, 0 \leqslant t \leqslant T, i, j = 1, 2, ..., N\}$. Based on the above considerations, our optimization problem is given as

$$J = \int_0^T (J_1(t) + J_2(t))\, \mathrm{d}t, \tag{3.9}$$

J. Stat. Mech. (2018) 123402

where

$$J_1(t) = \sum_{i=1}^{N} c_i p_i^L(t), J_2(t) = \frac{1}{2}\sum_{i=1}^{N}\sum_{j=1}^{N} d_{ij}\left(\mu_{ij}(t) - \mu_{ij}^0\right)^2, \tag{3.10}$$

subject to (2.5) with initial conditions $p_i^S(0) = p_0^S(i),\ p_i^{I_1}(0) = p_0^{I_1}(i),\ p_i^{I_2}(0) = p_0^{I_2}(i),\ p_i^L(0) = p_0^L(i),\ i, j = 1, 2, ..., N.$

3.1. The existence of the optimal control

In this part, we discuss the existence of a solution for the proposed optimal problem. We give the following theorem.

Theorem 3.1. *There exists a set of optimal weighted coefficient controls* $\mu_{ij}^*(t), i, j = 1, 2, ..., N$ *and corresponding solutions* $p_i^{S^*}(t), p_i^{I_1{}^*}(t), p_i^{I_2{}^*}(t), p_i^{L^*}(t), \forall i = 1, 2, ..., N$ *such that* $J(\mu_{ij}^*(t)) = \min\{J(\mu_{ij}(t))\}, i, j = 1, 2, ..., N.$

Proof. The theorem can be proved by the Cesari theorem [41], which satisfies the following arguments.

(1) The set of controls and state variables is non-empty;

(2) The control space is closed and convex;

(3) The right side of the system is bounded by a linear function with the state and control;

(4) The integrand in the objective function is convex with respect to the controls $\mu_{ij}, i = 1, 2, ..., N$;

(5) There exists a constant $C_1 > 1$ and positive numbers C_2 and C_3 such that

$$J(\mu_{ij}(t)) \geqslant C_2(\sum_{i=1}^{N} |\mu_{ij}(t)|^2)^{\frac{C_1}{2}} - C_3, \forall i = 1, 2, ..., N.$$

Next, we will prove that the SI_1I_2RL model satisfies the above five conditions. Obviously, if the system is uniformly Lipschitz continuous, the sets of Q^C and solutions to initial values are non-empty. Besides, state variables $p^S(t),\ p^{I_1}(t),\ p^{I_2}(t),\ p^L(t)$ are non-empty such that condition (1) is satisfied. The characteristics of control space and objective function can be verified by definition, meeting conditions (2) and (4). Condition (3) can be proved by the following discussion.

The system can be rewritten as

$$D(\phi) = \frac{\mathrm{d}\phi}{\mathrm{d}t} = B\phi + F(\phi), \tag{3.11}$$

where
$\phi = [\phi_1, \phi_2, ..., \phi_N] = [p^S(t), p^{I_1}(t), p^{I_2}(t), p^L(t)]^T, \phi_i = \left[p_i^S(t), p_i^{I_1}(t), p_i^{I_2}(t), p_i^L(t)\right]^T,$

$$p^S(t) = [p_1^S(t), p_2^S(t), ..., p_N^S(t)], p^{I_1}(t) = [p_1^{I_1}(t), p_2^{I_1}(t), ..., p_N^{I_1}(t)],$$

$$p^{I_2}(t) = [p_1^{I_2}(t), p_2^{I_2}(t), ..., p_N^{I_2}(t)], p^L(t) = [p_1^L(t), p_2^L(t), ..., p_N^L(t)].$$

$$B = \begin{pmatrix} 0 & 0 & 0 & 0 \\ 0 & -\gamma_1 & 0 & 0 \\ 0 & 0 & -\gamma_2 & 0 \\ 0 & 0 & 0 & 0 \end{pmatrix}, F(\phi_i) = \begin{pmatrix} -p_i^S(t) \sum_{j=1}^N \omega_{ij}(t) \left(\beta_1 p_j^{I_1}(t) + \beta_2 p_j^{I_2}(t)\right) \\ \sum_{j=1}^N \omega_{ij}(t) \left(\beta_1 p_j^{I_1}(t)\, p_i^S(t) - \beta_2 p_j^{I_2}(t)\, p_i^{I_1}(t)\right) \\ \sum_{j=1}^N \omega_{ij}(t) \left(\beta_2 p_j^{I_2}(t)\, p_i^S(t) - \beta_1 p_j^{I_1}(t)\, p_i^{I_2}(t)\right) \\ \sum_{j=1}^N \omega_{ij}(t) \left(\beta_2 p_j^{I_2}(t)\, p_i^{I_1}(t) + \beta_1 p_j^{I_1}(t)\, p_i^{I_2}(t)\right) \end{pmatrix}.$$

Thus, we can obtain

$$\begin{aligned}
|F(\phi_{i1}) - F(\phi_{i2})| &= \left| \sum_{z=1}^{2} \sum_{j=1}^{N} \omega_{ij}(t) \left\{ \beta_z \left(p_i^{S'}(t)\, p_j^{I_z\prime}(t) - p_i^S(t)\, p_j^{I_z}(t) \right) \right\} \right| \\
&+ \left| \sum_{j=1}^{N} \omega_{ij}(t) \left\{ \beta_1 \left(p_i^S(t)\, p_j^{I_1}(t) - p_i^{S'}(t)\, p_j^{I_1\prime}(t) \right) + \beta_2 \left(p_i^{I_1\prime}(t)\, p_j^{I_2\prime}(t) - p_i^{I_1}(t)\, p_j^{I_2}(t) \right) \right\} \right| \\
&+ \left| \sum_{j=1}^{N} \omega_{ij}(t) \left\{ \beta_2 \left(p_i^S(t)\, p_j^{I_2}(t) - p_i^{S'}(t)\, p_j^{I_2\prime}(t) \right) + \beta_1 \left(p_i^{I_2\prime}(t)\, p_j^{I_1\prime}(t) - p_i^{I_2}(t)\, p_j^{I_1}(t) \right) \right\} \right| \\
&+ \left| \sum_{j=1}^{N} \omega_{ij}(t) \left\{ \beta_2 \left(p_i^{I_1}(t)\, p_j^{I_2}(t) - p_i^{I_1\prime}(t)\, p_j^{I_2\prime}(t) \right) + \beta_1 \left(p_i^{I_2\prime}(t)\, p_j^{I_1\prime}(t) - p_i^{I_2}(t)\, p_j^{I_1}(t) \right) \right\} \right| \\
&\leqslant \sum_{z=1}^{2} \sum_{j=1}^{N} 2\beta_z \omega_{ij}(t)\, p_j^{I_z}(t) \left| p_i^S(t) - p_i^{S'}(t) \right| + 2\beta_2 \sum_{j=1}^{N} \omega_{ij}(t)\, p_j^{I_2}(t) \left| p_i^{I_1}(t) - p_i^{I_1\prime}(t) \right| \\
&+ 2\beta_1 \sum_{j=1}^{N} \omega_{ij}(t)\, p_j^{I_1}(t) \left| p_i^{I_2}(t) - p_i^{I_2\prime}(t) \right| + 2 \sum_{j=1}^{N} \left(\beta_1 p_i^{S'}(t) + \beta_1 p_i^{I_2\prime}(t) \right) \omega_{ij}(t) \left| p_j^{I_1}(t) - p_j^{I_1\prime}(t) \right| \\
&+ 2 \sum_{j=1}^{N} \left(\beta_2 p_i^{S'}(t) + \beta_2 p_i^{I_1\prime}(t) \right) \omega_{ij}(t) \left| p_j^{I_2}(t) - p_j^{I_2\prime}(t) \right| \triangleq M_i.
\end{aligned}$$

Then

$$\begin{aligned}
|F(\phi_1) - F(\phi_2)| &= \sum_{i=1}^{N} |F(\phi_{i1}) - F(\phi_{i2})| \leqslant \sum_{i=1}^{N} M_i \leqslant 2(\beta_1 + \beta_2)(N-1) \left| p^S(t) - p^{S'}(t) \right| \\
&+ 2(\beta_2 + \beta_1 + \beta_1)(N-1) \left| p^{I_1}(t) - p^{I_1\prime}(t) \right| + 2(\beta_2 + \beta_1 + \beta_2)(N-1) \left| p^{I_2}(t) - p^{I_2\prime}(t) \right| \\
&\leqslant Q \left(\left| p^S(t) - p^{S'}(t) \right| + \left| p^{I_1}(t) - p^{I_1\prime}(t) \right| + \left| p^{I_2}(t) - p^{I_2\prime}(t) \right| + \left| p^L(t) - p^{L'}(t) \right| \right),
\end{aligned}$$

where

$$Q = \max\left\{2(\beta_1 + \beta_2)(N-1), 2(\beta_2 + 2\beta_1)(N-1), 2(2\beta_2 + \beta_1)(N-1)\right\}.$$

Thus, we have

$$|D(\phi_1) - D(\phi_2)| \leqslant V \left|\phi_1 - \phi_2\right|,$$

where

$$V = \max\left\{Q, \|B\|\right\} \leqslant \infty,$$

J. Stat. Mech. (2018) 123402

which leads to the fact that the function D is uniformly Lipschitz continuous (satisfying the assumption of condition (1)) and satisfies the required bound of the Cesari theorem. The set of weighted coefficients belongs to the closed set $[0,1]$ and the value of the objective function in equation (3.9) lies in an interval $[J_{\min}, J_{\max}]$. Hence the function D is linear in $\mu_{ij}(t), i,j = 1,2,...,N$. Condition (3) is satisfied. As a result, we can draw the conclusion that the solution of the system exists.

Furthermore, we have

$$\begin{aligned}
&\frac{1}{2}\sum_{i=1}^{N}\sum_{j=1}^{N} d_{ij}(\mu_{ij}(t)-\mu_{ij}^{0})^{2} = \frac{1}{2}\sum_{i=1}^{N}\sum_{j=1}^{N} d_{ij}((\mu_{ij}(t))^{2} - 2\mu_{ij}(t)\mu_{ij}^{0} + (\mu_{ij}^{0})^{2}) \\
&\geqslant \frac{1}{2}\min\{d_{ij}\}(\sum_{i=1}^{N}\sum_{j=1}^{N}|\mu_{ij}(t)|^{2} - \sum_{i=1}^{N}\sum_{j=1}^{N}(2\mu_{ij}(t)\mu_{ij}^{0} - (\mu_{ij}^{0})^{2})) \\
&\geqslant \frac{1}{2}\min\{d_{ij}\}(\sum_{i=1}^{N}\sum_{j=1}^{N}|\mu_{ij}(t)|^{2}) - \frac{1}{2}\min\{d_{ij}\}[\sum_{i=1}^{N}\sum_{j=1}^{N}(2-(\mu_{ij}^{0})^{2})] \\
&\geqslant \frac{1}{2}\min\{d_{ij}\}(\sum_{i=1}^{N}\sum_{j=1}^{N}|\mu_{ij}(t)|^{2}) - \frac{1}{2}\min\{d_{ij}\}N^{2}[2-(\min\{\mu_{ij}^{0}\})^{2}].
\end{aligned}$$

Let $C_2 = \frac{1}{2}\min\{d_{ij}\} > 0, C_1 = 2, C_3 = \frac{1}{2}\min\{d_{ij}\}N^2[2-(\min\{\mu_{ij}^0\})^2] > 0$, then

$$J(\mu_{ij}(t)) \geqslant C_2(\sum_{i=1}^{N}\sum_{j=1}^{N}|\mu_{ij}(t)|^{2})^{\frac{C_1}{2}} - C_3, \forall i = 1,2,...,N$$

has been satisfied, which means the optimal solution exists.

In summary, the proof of theorem 3.1 has been completed.

3.2. Solution to the optimal control problem

In this part, our objective is to solve the optimal control problem using Hamiltonian methods and Pontryagin's maximum principle with fixed final time. Obviously, according to the objective function (3.9), the Lagrangian of the optimal problem can be formed as

$$L = \sum_{i=1}^{N} c_i p_i^L(t) + \frac{1}{2}\sum_{i=1}^{N}\sum_{j=1}^{N} d_{ij}(\mu_{ij}(t)-\mu_{ij}^{0})^{2}. \tag{3.12}$$

Define $\lambda(t) = (\lambda_1(t), \lambda_2(t), \lambda_3(t), \lambda_4(t)), \lambda_j(t) = (\lambda_{j1}(t), \lambda_{j2}(t), ..., \lambda_{jN}(t))^T, j = 1,2,3,4$ as costate variables, then we can derive the corresponding Hamiltonian function of (3.12) as

$$\begin{aligned}
H = &\sum_{i=1}^{N} c_i p_i^L(t) + \frac{1}{2}\sum_{i=1}^{N}\sum_{j=1}^{N} d_{ij}(\mu_{ij}(t)-\mu_{ij}^{0})^{2} \\
&+ \sum_{i=1}^{N}\left(\lambda_{1i}(t)\dot{p}_i^S(t) + \lambda_{2i}(t)\dot{p}_i^{I_1}(t) + \lambda_{3i}(t)\dot{p}_i^{I_2}(t) + \lambda_{4i}(t)\dot{p}_i^L(t)\right).
\end{aligned} \tag{3.13}$$

Next, we are in a position to discuss the solution of the proposed weighted coefficient optimization problem according to the following theorem.

Theorem 3.2. *There is optimal control of weighted coefficient* $\mu_{ij}^{*}(t)$ *given as*

$$\mu_{ij}^{*}(t)=\min\left\{\max\left\{0,\mu_{ij}^{0}-\frac{Z_{ij}(t)}{d_{ij}+d_{ji}}\right\},1\right\}, \tag{3.14}$$

where

$$\begin{aligned}Z_{ij}(t)=&\sum_{\substack{(\nu,\kappa)=(i,j)\\(\nu,\kappa)=(j,i)}}\xi_{ij}(t)\left\{p_{\kappa}^{I_1}(t)\left[\beta_1 p_{v}^{S}(t)\left(\lambda_{2\nu}(t)-\lambda_{1\nu}(t)\right)+\beta_1 p_{\nu}^{I_1}(t)\left(\lambda_{4\nu}(t)-\lambda_{3\nu}(t)\right)\right]\right.\\&\left.+p_{\kappa}^{I_2}(t)\left[\beta_2 p_{\nu}^{S}(t)\left(\lambda_{3\nu}(t)-\lambda_{1\nu}(t)\right)+\beta_2 p_{\nu}^{I_2}(t)\left(\lambda_{4\nu}(t)-\lambda_{2\nu}(t)\right)\right]\right\},\end{aligned} \tag{3.15}$$

$$\xi_{ij}(t)=\frac{\mathrm{d}\omega_{ij}(t)}{\mathrm{d}\mu_{ij}(t)}=x_{ij}(t)-x_{ji}(t). \tag{3.16}$$

Costate variables $\lambda_{1i}(t),\lambda_{2i}(t),\lambda_{3i}(t),\lambda_{4i}(t),\forall i=1,2,...,N$ *satisfy*

$$\begin{aligned}\dot{\lambda}_{1i}(t)=&\left(\lambda_{1i}(t)-\lambda_{2i}(t)\right)\sum_{j=1}^{N}\beta_1 p_{j}^{I_1}(t)\omega_{ij}(t)+\left(\lambda_{1i}(t)-\lambda_{3i}(t)\right)\sum_{j=1}^{N}\beta_2 p_{j}^{I_2}(t)\omega_{ij}(t),\\
\dot{\lambda}_{2i}(t)=&\sum_{z=2}^{3}\left(\lambda_{1i}(t)-\lambda_{zi}(t)\right)p_{i}^{S}(t)\beta_{z-1}\sum_{j=1}^{N}\delta_{1ij}(t)\,p_{j}^{I_{z-1}}(t)\\
&+\sum_{j=1}^{N}\left\{\beta_1\left(\lambda_{1j}(t)-\lambda_{2j}(t)\right)\delta_{2ij}(t)+\beta_2 p_{i}^{I_2}(t)\left(\lambda_{1j}(t)-\lambda_{3j}(t)\right)\delta_{1ij}(t)\right\}p_{j}^{S}(t)\\
&+\sum_{j=1}^{N}\left\{p_{i}^{I_2}(t)\left(\beta_1\left(\lambda_{3i}(t)-\lambda_{4i}(t)\right)+\beta_2\left(\lambda_{2j}(t)-\lambda_{4j}(t)\right)\right)\right\}\delta_{1ij}(t)\,p_{j}^{I_1}(t)\\
&+\sum_{j=1}^{N}\left\{\beta_2\left(\lambda_{2i}(t)-\lambda_{4i}(t)\right)+\beta_1\left(\lambda_{3j}(t)-\lambda_{4j}(t)\right)\right\}\delta_{2ij}(t)\,p_{j}^{I_2}(t)+\lambda_{2i}(t)\gamma_1,\\
\dot{\lambda}_{3i}(t)=&\sum_{z=2}^{3}\left(\lambda_{1i}(t)-\lambda_{zi}(t)\right)p_{i}^{S}(t)\beta_{z-1}\sum_{j=1}^{N}\delta_{1ij}(t)\,p_{j}^{I_{z-1}}(t)\\
&+\sum_{j=1}^{N}\left\{\beta_1 p_{i}^{I_1}(t)\left(\lambda_{1j}(t)-\lambda_{2j}(t)\right)\delta_{1ij}(t)+\beta_2\left(\lambda_{1j}(t)-\lambda_{3j}(t)\right)\delta_{3ij}(t)\right\}p_{j}^{S}(t)\\
&+\sum_{j=1}^{N}\left\{\beta_1\left(\lambda_{3i}(t)-\lambda_{4i}(t)\right)+\beta_2\left(\lambda_{2j}(t)-\lambda_{4j}(t)\right)\right\}\delta_{3ij}(t)\,p_{j}^{I_1}(t)+\lambda_{3i}(t)\gamma_2\\
&+\sum_{j=1}^{N}\left\{p_{i}^{I_1}(t)\left(\beta_2\left(\lambda_{2i}(t)-\lambda_{4i}(t)\right)+\beta_1\left(\lambda_{3j}(t)-\lambda_{4j}(t)\right)\right)\right\}\delta_{1ij}(t)\,p_{j}^{I_2}(t),\\
\dot{\lambda}_{4i}(t)=&-c_i,\end{aligned}$$

where

$$\begin{cases} \delta_{1ij}(t)=\frac{\partial\omega_{ij}(t)}{\partial p_i^{I_1}(t)} = \frac{\partial\omega_{ij}(t)}{\partial p_i^{I_2}(t)} = -\frac{(1-\mu_{ij}(t))x_{ji}^0}{1-\mathrm{e}^{-\eta_j}}\mathrm{e}^{\psi_{ji}(t)-\eta_j}, \\ \delta_{2ij}(t) = \frac{\partial\left[p_i^{I_1}(t)\omega_{ij}(t)\right]}{\partial p_i^{I_1}(t)} = \omega_{ij}(t) - \frac{(1-\mu_{ij}(t))x_{ji}^0}{1-\mathrm{e}^{-\eta_j}}p_i^{I_1}(t)\mathrm{e}^{\psi_{ji}(t)-\eta_j}, \\ \delta_{3ij}(t) = \frac{\partial\left[p_i^{I_2}(t)\omega_{ij}(t)\right]}{\partial p_i^{I_2}(t)} = \omega_{ij}(t) - \frac{(1-\mu_{ij}(t))x_{ji}^0}{1-\mathrm{e}^{-\eta_j}}p_i^{I_2}(t)\mathrm{e}^{\psi_{ji}(t)-\eta_j}, \end{cases} \tag{3.17}$$

with transversality conditions

$$\lambda_1(T) = \lambda_2(T) = \lambda_3(T) = \lambda_4(T) = 0. \tag{3.18}$$

Proof. While characterizing the properties of the optimal solution, the costate conditions must be satisfied in the system of costate differential equations as

$$\dot{\lambda}_{1i} = -\frac{\partial H}{\partial p_i^S(t)}, \dot{\lambda}_{2i} = -\frac{\partial H}{\partial p_i^{I_1}(t)}, \dot{\lambda}_{3i} = -\frac{\partial H}{\partial p_i^{I_2}(t)}, \dot{\lambda}_{4i} = -\frac{\partial H}{\partial p_i^L(t)}.$$

Then, by the optimal conditions, we have

$$\frac{\partial H}{\partial \mu_{ij}(t)} = (d_{ij} + d_{ji})\left(\mu_{ij}(t) - \mu_{ij}^0\right) + Z_{ij}(t),$$

of which $Z_{ij}(t)$ has been defined in equation (3.15).

Let $\frac{\partial H}{\partial \mu_{ij}(t)} = 0$, so we can obtain the optimal weighted coefficient at time t satisfying

$$\mu_{ij}^*(t) = \mu_{ij}^0 - \frac{Z_{ij}(t)}{d_{ij} + d_{ji}}.$$

Considering the property of the control space, we obtain

$$\mu_{ij}^*(t) = \begin{cases} 0, & \text{if } \mu_{ij}^0 - \frac{Z_{ij}(t)}{d_{ij}+d_{ji}} \leqslant 0, \\ \mu_{ij}^0 - \frac{Z_{ij}(t)}{d_{ij}+d_{ji}}, & \text{if } 0 < \mu_{ij}^0 - \frac{Z_{ij}(t)}{d_{ij}+d_{ji}} < 1, \\ 1, & \text{if } \mu_{ij}^0 - \frac{Z_{ij}(t)}{d_{ij}+d_{ji}} \geqslant 1. \end{cases}$$

Thus we have the optimal weighted coefficient $\mu_{ij}^*(t)$ in compact notation

$$\mu_{ij}^*(t) = \min\left\{\max\left\{0, \mu_{ij}^0 - \frac{Z_{ij}(t)}{d_{ij} + d_{ji}}\right\}, 1\right\}.$$

In summary, the proof of theorem 3.2 has been completed.

Remark 3.1. Mathematical expression (3.14) reveals the characterization of the optimal control variable, through which it can be found that the optimal weighted coefficient is the time-varying result on the basis of its initial value. And the variation of weighted coefficient $|Z_{ij}(t)/(d_{ij} + d_{ji})|$ conforms to a complicated rule associated with an individual's state and expected weight, costate variables, the coefficient of cost, among which the variables with time-varying characteristics are also constrained by static network topology and determined terminal time. Note that at time T, we have

J. Stat. Mech. (2018) 123402

$\lambda_i = 0$ for all i, thus $Z_{ij}(T) = 0$, representing that the optimal weighted coefficient may return to its initial value at terminal. Besides, since the states and costate variables are all bounded, and system (2.5) satisfies Lipschitz structure, the uniqueness of the optimal solution can be guaranteed for small T.

4. Numerical experiments and analysis

In this section, we present numerical simulations by introducing two examples with different network size to demonstrate theoretical results of the optimal weighted coefficient problem.

4.1. Example 1

In this example, for the purposes of verifying the result of the optimal control problem, a weighted undirected BA scale-free network that consists of 500 nodes and 4871 edges is constructed, which has a power law degree distribution $p_k = \sigma k^{-\upsilon}$. Specifically, σ normalizes the distribution to 1, k is defined as the degree among individuals and the power law exponent is chosen as $\upsilon = 2.713$. The minimum and maximum degrees among all individuals are $k_{\min} = 10$ and $k_{\max} = 93$. In order to characterize the heterogeneity of individuals, their probabilities in infected states, sensitivity coefficients and initial expected weights towards neighbors are randomly selected, satisfying $p_i^{I_1}(0) \in [0, 0.2], p_i^{I_2}(0) \in [0, 0.2], \eta_i \in [0.45, 1.55], x_{ij}^0 \in [0, 1]$ for $i, j = 1, 2, ..., N$. It is proved that the randomness of initial infection probability, sensitivity coefficient and initial expected weight will not affect the results of the proposed problem through a large number of simulation experiments. Besides, take the same initial values $p_i^L(0) = p_i^R(0) = 0$ for all individuals, and thus $p_i^S(0) = 1 - p_i^{I_1}(0) - p_i^{I_2}(0)$. The density of individuals in susceptible, infected by pathogen 1, infected by pathogen 2, limited and recovered states at time t is represented by $V_s(t), V_{i1}(t), V_{i2}(t), V_l(t), V_r(t)$ respectively, then $V_s(t) = \sum_{i=1}^N p_i^S(t), V_{i1}(t) = \sum_{i=1}^N p_i^{I_1}(t), V_{i2}(t) = \sum_{i=1}^N p_i^{I_2}(t), V_l(t) = \sum_{i=1}^N p_i^L(t), V_r(t) = \sum_{i=1}^N p_i^R(t)$, and thus we have $V_s(0) = 0.8046, V_{i1}(0) = 0.0972, V_{i2}(0) = 0.0982, V_l(0) = 0, V_r(0) = 0$. Let spreading parameters $\beta_1 = 0.20$, $\beta_2 = 0.22$, $\gamma_1 = 0.080$, $\gamma_2 = 0.085$. The coefficients of infection and weighted coefficient adjustment cost c_i, d_{ij} are set to be $c_i = 1.0$ and $d_{ij} = 0.2$ for $i, j = 1, 2, ..., N$. In addition, the initial weighted coefficient μ_{ij}^0 is chosen as 0.5 for all individuals and the terminal time is chosen as $T = 30$. The forward–backward sweep algorithm [42] is adopted for solving the optimal weighted coefficient adjustment problem, which can be illustrated as follows.

- Firstly, states are solved forward in time with initial conditions and initial guesses for weighted coefficients;
- Secondly, costate variables with transversality conditions are solved backward in time;
- Thirdly, optimal weighted coefficients are updated;

J. Stat. Mech. (2018) 123402

- Finally, the three steps above are iterated until convergence is achieved.

To assess the performance of the proposed control mechanism, we introduce the following heuristic control strategy that contains the feedback information about the current expected weights of each individual.

$$\mu_{ij}(t) = \mu_{ij}^0 + \Delta C \rho_{ij}(t), \Delta C > 0, \tag{4.1}$$

where $\rho_{ij}(t) = \operatorname{sgn}\{x_{ji}(t) - x_{ij}(t)\}$, is a symbol coefficient that determines whether the weighted coefficient of individual i towards neighbor j increases or decreases. It is obvious that whether $\rho_{ij}(t)$ is positive or negative depends on the relative magnitude of the expected weights of individual i and neighbor j. Specifically, an individual i's expected weight is lower than that of their neighbor j, which means that either individual i's aversion tendency or neighbor j's infection level is high. Then individual i's willingness to connect or communicate may occupy a more dominant position, making contact weight more inclined to individual i's expected weight and decrease compared to its initial value, and vice versa.

Note that the value of ΔC is arbitrary if it lies in the interval $\left[0, \min\left\{\mu_{ij}^0, \mu_{ji}^0\right\}\right]$. Here we choose $\Delta C = 0.4$. In figure 5, the cumulative and instantaneous cost under optimal control strategy, heuristic control strategy and no control strategy between $[0, T]$ are compared. For cumulative cost, it is observed from figure 5(a) that total cost is always the highest under heuristic control. This is because heuristic control is a strategy that pays more attention to control performance regardless of cost, which also makes the adjustment cost of heuristic control higher than that of optimal control, as shown in figure 5(c). There is a crossover between the total cost lines of optimal control and no control at $t = 14.318$; optimal control may have higher total cost initially while the situation will reverse after crossover. Besides, as shown in figure 5(b), due to the adoption of appropriate measures, optimal and heuristic control can reduce the infection cost under no control effectively and the control effect of the latter is more significant. For instantaneous cost, from total cost curves in figure 5(d), both heuristic control and no control cross over with optimal control, at $t = 0.326$ and $t = 5.092$ respectively. After crossovers, optimal control can maintain the lowest total cost. In figure 5(f), we can see that the adjustment cost of optimal control presents a monotonic downward trend and eventually reaches zero. But heuristic control does not cause cost fluctuations, meaning that the adjustment cost is always constant over time. The phenomenon in figure 5(e) is similar to that in figure 5(b).

Furthermore, the densities of individuals in each state over time are provided in figure 6. It is not hard to see that heuristic and optimal control strategies can play significant roles in restricting adverse states. To be specific, under two effective control strategies there will be more susceptible and recovered individuals but fewer limited individuals, as shown in figures 6(a), (d) and (e). Owing to higher control cost, heuristic strategy performs better than optimal strategy. In figures 6(b) and (c), note that compared to the other two strategies, the densities of individuals infected by pathogen 1 and 2 under no control may be higher initially and lower later. This is mainly because the introduction of two control strategies changes the contact weights between individuals, then the spreading process is influenced: (1) the connection between infected and susceptible individuals may be reduced, thereby decreasing the probability that

J. Stat. Mech. (2018) 123402

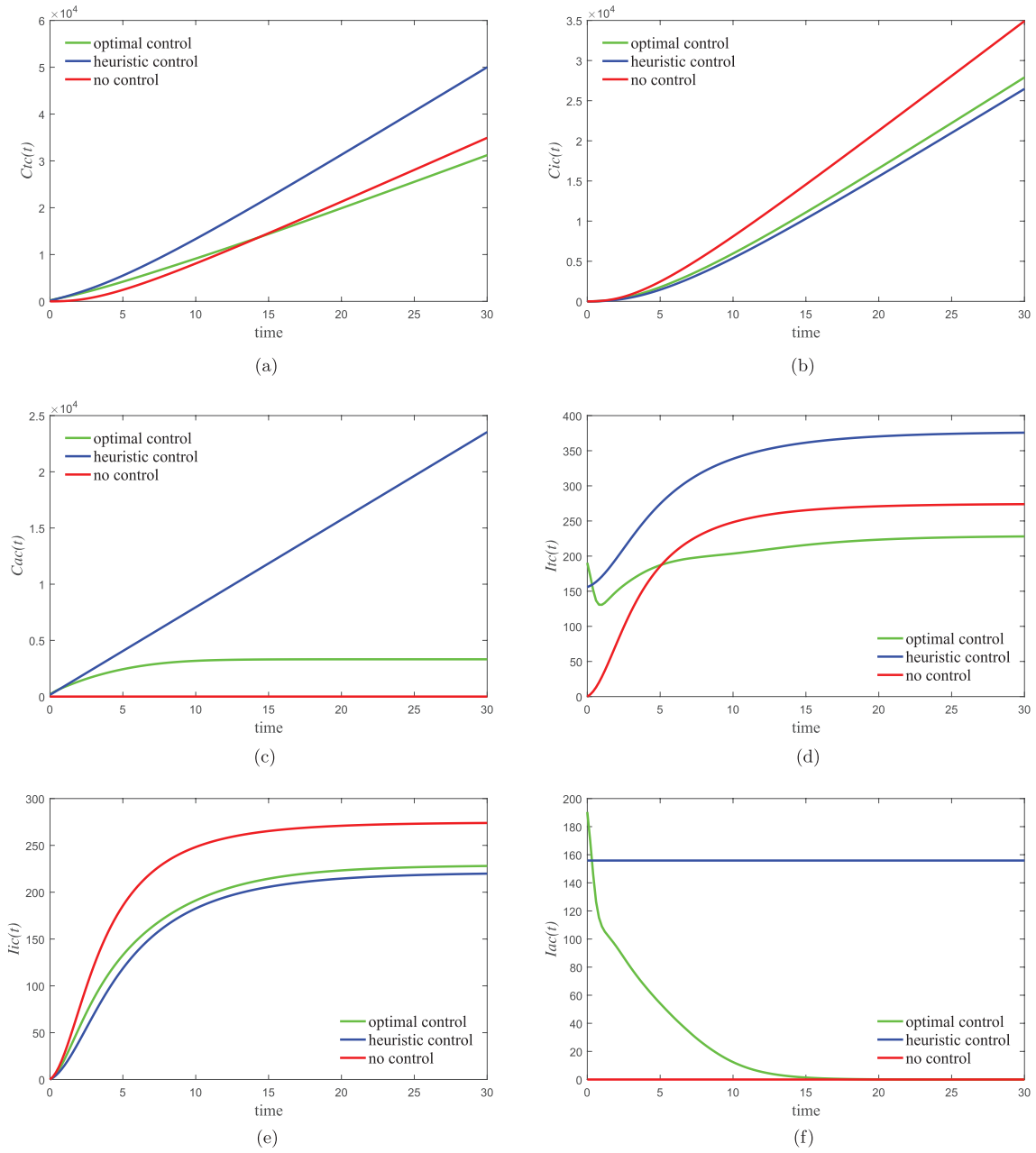

Figure 5. The cumulative and instantaneous cost under different control mechanisms over time. (a) Ctc versus t (Ctc represents cumulative total cost). (b) Cic versus t (Cic represents cumulative infection cost). (c) Cac versus t (Cac represents cumulative adjustment cost). (d) Itc versus t (Itc represents instantaneous total cost). (e) Iic versus t (Iic represents instantaneous infection cost). (f) Iac versus t (Iac represents instantaneous adjustment cost).

susceptible individuals become infected; and (2) the connection between infected individuals may be also reduced, which blocks the formation channels of limited individuals, making more infected individuals transform into the recovery state naturally.

J. Stat. Mech. (2018) 123402

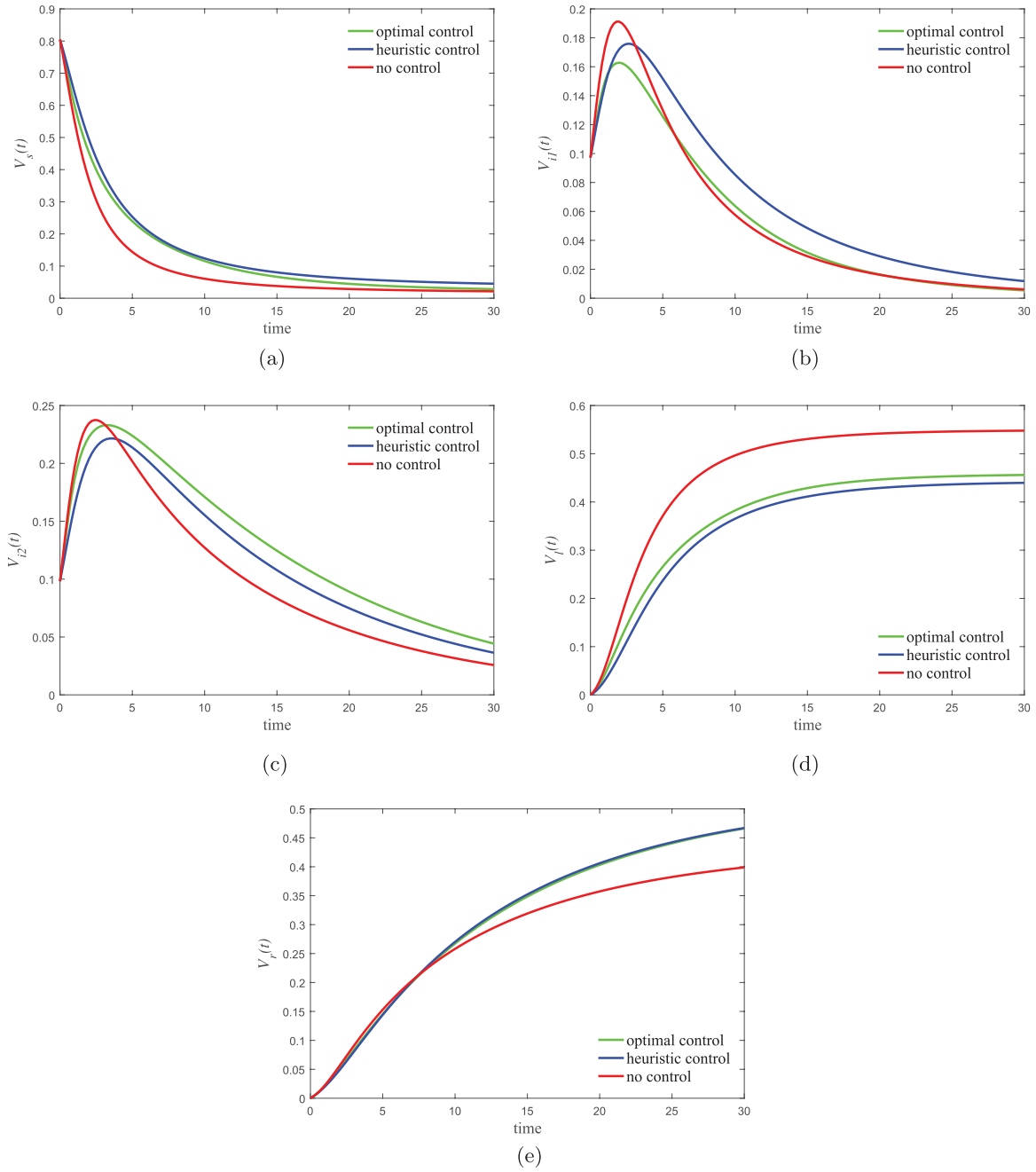

Figure 6. The density of individuals in each state under different control strategies over time. (a) V_s versus t. (b) V_{i1} versus t. (c) V_{i2} versus t. (d) V_l versus t. (e) V_r versus t.

4.2. Example 2

In this example, in order to deeply elaborate the dynamical evolution of the network reflecting individual behavior under optimal mechanism, a weighted undirected small-scale network that consists of 40 nodes and 560 edges is constructed. The minimum and maximum degree among all individuals are $k_{\min} = 17$ and $k_{\max} = 37$. Here we deliberately reduce the heterogeneity of individuals aiming to more clearly observe

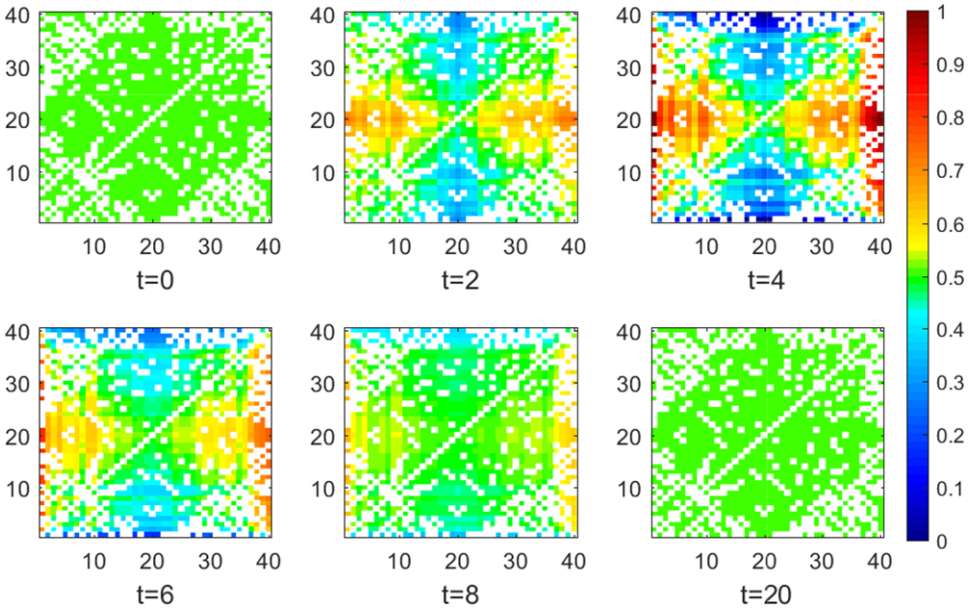

Figure 7. The patterns of weighted coefficients relating to individuals in the network at different simulation times. (Each individual is numbered according to their degree, where the larger the degree is, the closer to the middle the number assigned is. The numbers along the x-axis and y-axis in each subgraph are the numberings of all individuals. Each square in the subgraph represents the weighted coefficient relating to the connected individuals. White squares indicate that the two individuals are not connected in the initial network topology, and the values corresponding to the squares of other colors are shown in the color map.)

the changes in individual behavior over time. Thus, take the same initial values $p_i^S(0) = 0.5$, $p_i^{I_1}(0) = p_i^{I_2}(0) = 0.25$, $p_i^L(0) = p_i^R(0) = 0$ for each individual. Spreading parameters are set as $\beta_1 = 0.05$, $\beta_2 = 0.06$, $\gamma_1 = 0.1$, $\gamma_2 = 0.09$. Sensitivity coefficients, initial expected weights and initial weighted coefficients of all individuals remain homogeneous, as $\eta_i = 1.0$, $x_{ij}^0 = 1.0$, $\mu_{ij}^0 = 0.5$, which makes the initial contact weight equal to 0.6225, for $i, j = 1, 2, ..., N$. Besides, let cost coefficients $c_i = 0.8$, $d_{ij} = 0.003$ and terminal time $T = 20$. The same optimization algorithm as in example 1 is utilized.

Firstly, we observe the dynamical evolution of individual behavior from the perspective of weighted coefficients. For the purpose of achieving the goal of minimizing total cost, individuals' weighted coefficients may be adjusted accordingly due to the time-varying characteristics of individuals' states. Owing to the homogeneous setting of initial parameters, the heterogeneity of individuals is mainly determined by network topology. In figure 7, the patterns of weighted coefficients relating to connected individuals at different time are presented, and are assigned in accordance with an individual's degree. As we can see, individuals with small degree are more likely to adjust their weighted coefficients. Their connections with neighbors whose degree is large will make their weighted coefficients change earlier and will be biased to 0 and 1 over time. However, individuals with large degree may only adjust their weighted coefficients towards the neighbors with small degree, and there is almost no adjustment of weighted coefficients towards the neighbors whose degree is close to their own. All individuals' weighted coefficients will gradually recover and go back to the

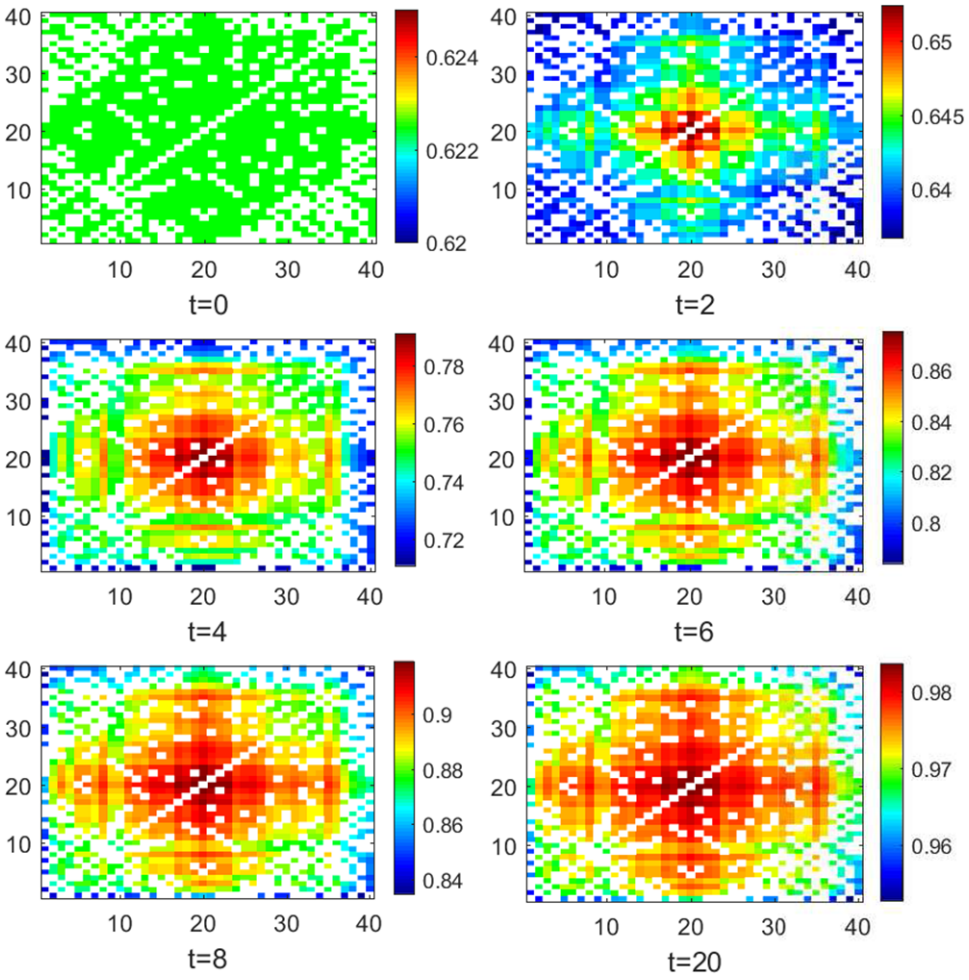

Figure 8. The patterns of contact weight between any two individuals in the network at different simulation times. (The numbers along the x-axis and y-axis in each subgraph are the numberings of all individuals with the same means as figure 7. Each square in the subgraph represents the contact weight between two individuals. White squares indicate that the two individuals are not connected in the initial network topology, and the values corresponding to the squares of other colors are shown in the color map. Obviously, each subgraph is symmetrical about the diagonal.)

original value at terminal time T, which is consistent with the theoretical analysis of remark 3.1. These results indicate that under optimal mechanism, individuals' adjustment behaviors are affected by network topology, especially degree difference between individuals.

Next, we discuss the evolutionary trend of individuals' contact weight in an epidemic spreading process. The adjustment of weighted coefficient is reflected in the change of contact weight between individuals, and the individual behaviors of adjusting weighted coefficients have been presented in figure 7, which can be a basis for analyzing the evolution of contact weights. Furthermore, in order to observe the influence of such behaviors on contact weights intuitively, the patterns of contact weights at varying time are shown in figure 8. As time goes by, contact weights may increase because the

attenuation of infection density may lead to a rise of individuals' expected weights. At each moment, for individuals with large degree, if the degree difference between them and their neighbor is smaller, their contact weight will be larger. However, it is exactly the opposite for individuals with small degree.

In a word, we would like to utilize this example to characterize how individuals should behave under the optimal mechanism aiming to minimize total cost. The conclusion that when the initial values of all individuals is homogeneous, the optimal solution of individual behavior is mainly affected by network topology can be drawn.

5. Conclusion

In this paper, we have presented the optimal control problem of weighted coefficient in a heterogeneous epidemic spreading network to assess the trade-off between the global infection level and each individual's weighted coefficient adjustment. The existence of an optimal solution is proved and the general structure of optimal weighted coefficient for each individual is provided. We conducted a series of numerical experiments to verify our theoretical results. Comparison of costs under the optimal control strategy, heuristic control strategy and no control strategy was made and it was proved that the optimal control strategy is more effective than other strategies at minimizing the proposed cost function. Furthermore, the time-varying weighted network reflected by the evolution of weighted coefficient and contact weight was presented, through which individual dynamical behavior can be seen under the optimal mechanism. It can be concluded that the selection of optimal individual behavior may be affected by degree difference, which reflects the impact of network topology on the spreading process. In future work, we may focus on the distributed optimization problems and the design of expected weight with more factors taken into account.

In conclusion, our study can reflect the relationship between network topology, epidemic spreading and individual behavior adjustment within the framework of optimal weighted coefficient control, which may provide useful insights for other applications such as rumor, information and computer virus propagation.

Acknowledgments

This work was supported by National Natural Science Foundation of China under Grant 61873194.

References

[1] Huang Y, Ding L, Feng Y and Pan J 2016 Epidemic spreading in random walkers with heterogeneous interaction radius *J. Stat. Mech.* 103501

[2] Elaiw A M and AlShamrani N H 2015 Global stability of humoral immunity virus dynamics models with nonlinear infection rate and removal *Nonlinear Anal. Real World Appl.* **26** 161–90

[3] Tang C and Wu Y 2017 Global exponential stability of nonresident computer virus models *Nonlinear Anal. Real World Appl.* **34** 149–58

J. Stat. Mech. (2018) 123402

[4] Cheng C, Dong Y and Takeuchi Y 2018 An age-structured virus model with two routes of infection in heterogeneous environments *Nonlinear Anal. Real World Appl.* **39** 464–91
[5] Liu C and Zhang Z 2014 Information spreading on dynamic social networks *Commun. Nonlinear Sci. Numer. Simul.* **19** 896–904
[6] Jia F, Lv G, Wang S and Zou G 2018 Dynamic analysis of a stochastic delayed rumor propagation model *J. Stat. Mech.* 023502
[7] Wang C, Tan Z X, Ye Y, Wang L, Cheong K H and Xie N 2017 A rumor spreading model based on information entropy *Sci. Rep.* **7** 9615
[8] Zhao J, Li D, Sanhedrai H, Cohen R and Havlin S 2016 Spatio-temporal propagation of cascading overload failures in spatially embedded networks *Nat. Commun.* **7** 10094
[9] Moussawi A, Derzsy N, Lin X, Szymanski B K and Korniss G 2017 Limits of predictability of cascading overload failures in spatially-embedded networks with distributed flows *Sci. Rep.* **7** 11729
[10] Korkali M, Veneman J G, Tivnan B F, Bagrow J P and Hines P D 2017 Reducing cascading failure risk by increasing infrastructure network interdependence *Sci. Rep.* **7** 44499
[11] Tan Y, Huang C, Sun B and Wang T 2018 Dynamics of a class of delayed reaction–diffusion systems with Neumann boundary condition *J. Math. Anal. Appl.* **458** 1115–30
[12] Carrère C 2018 Spreading speeds for a two-species competition-diffusion system *J. Differ. Equ.* **264** 2133–56
[13] Jiang J and Zhou T 2018 Resource control of epidemic spreading through a multilayer network *Sci. Rep.* **8** 1629
[14] Liu W and Zhong S 2017 Web malware spread modelling and optimal control strategies *Sci. Rep.* **7** 42308
[15] Kang H and Fu X 2015 Epidemic spreading and global stability of an SIS model with an infective vector on complex networks *Commun. Nonlinear Sci. Numer. Simul.* **27** 30–9
[16] Huang D and Yu Z 2017 Dynamic-sensitive centrality of nodes in temporal networks *Sci. Rep.* **7** 41454
[17] Huo H, Yang P and Xiang H 2018 Stability and bifurcation for an SEIS epidemic model with the impact of media *Physica* A **490** 702–20
[18] Xu D, Xu X, Xie Y and Yang C 2017 Optimal control of an SIVRS epidemic spreading model with virus variation based on complex networks *Commun. Nonlinear Sci. Numer. Simul.* **48** 200–10
[19] Watkins N J, Nowzari C, Preciado V M and Pappas G J 2018 Optimal resource allocation for competitive spreading processes on bilayer networks *IEEE Trans. Control Netw. Syst.* **5** 298–307
[20] Karrer B and Newman M E 2011 Competing epidemics on complex networks *Phys. Rev.* E **84** 036106
[21] Darabi Sahneh F and Scoglio C 2014 Competitive epidemic spreading over arbitrary multilayer networks *Phys. Rev.* E **89** 062817
[22] Poletto C, Meloni S, Van Metre A, Colizza V, Moreno Y and Vespignani A 2015 Characterising two-pathogen competition in spatially structured environments *Sci. Rep.* **5** 7895
[23] Chen L, Ghanbarnejad F and Brockmann D 2017 Fundamental properties of cooperative contagion processes *New J. Phys.* **19** 103041
[24] Chen L, Ghanbarnejad F, Cai W and Grassberger P 2013 Outbreaks of coinfections: the critical role of cooperativity *Europhys. Lett.* **104** 50001
[25] Cui P, Colaiori F and Castellano C 2017 Mutually cooperative epidemics on power-law networks *Phys. Rev.* E **96** 022301
[26] Marceau V, Noel P A, Hebert Dufresne L, Allard A and Dube L J 2011 Modeling the dynamical interaction between epidemics on overlay networks *Phys. Rev.* E **84** 026105
[27] Azimi-Tafreshi N 2016 Cooperative epidemics on multiplex networks *Phys. Rev.* E **93** 042303
[28] Jia N, Ding L, Liu Y and Hu P 2018 Global stability and optimal control of epidemic spreading on multiplex networks with nonlinear mutual interaction *Physica* A **502** 93–105
[29] Kashirin V V and Dijkstra L J 2013 A heuristic optimization method for mitigating the impact of a virus attack *Procedia Comput. Sci.* **18** 2619–28
[30] Zhang H, Li K, Fu X and Wang B 2009 An efficient control strategy of epidemic spreading on scale-free networks *Chin. Phys. Lett.* **26** 68901
[31] Feng Y, Ding L, Huang Y and Zhang L 2016 Epidemic spreading on weighted networks with adaptive topology based on infective information *Physica* A **463** 493–502
[32] Feng Y, Ding L and Hu P 2018 Epidemic spreading on random surfer networks with optimal interaction radius *Commun. Nonlinear Sci. Numer. Simul.* **56** 344–53
[33] Taynitskiy V, Gubar E and Zhu Q 2017 Optimal impulsive control of epidemic spreading of heterogeneous malware *IFAC-PapersOnLine* **50** 15038–43
[34] Hu P, Ding L and Hadzibeganovic T 2018 Individual-based optimal weight adaptation for heterogeneous epidemic spreading networks *Commun. Nonlinear Sci. Numer. Simul.* **63** 339–55
[35] Shao F and Jiang G 2013 Optimal control strategy for traffic driven epidemic spreading based on community structure *Math. Problems Eng.* **2013** 1–10

J. Stat. Mech. (2018) 123402

[36] Eshghi S, Khouzani M H R, Sarkar S and Venkatesh S S 2016 Optimal patching in clustered malware epidemics *IEEE/ACM Trans. Netw.* **24** 283–98
[37] Chen X, Wang W, Cai S, Stanley H E and Braunstein L A 2018 Optimal resource diffusion for suppressing disease spreading in multiplex networks *J. Stat. Mech.* 053501
[38] Pan Y and Yan Z 2018 The impact of individual heterogeneity on the coupled awareness-epidemic dynamics in multiplex networks *Chaos* **28** 063123
[39] Chakrabarti D, Wang Y, Wang C, Leskovec J and Faloutsos C 2008 Epidemic thresholds in real networks *ACM Trans. Inf. Syst. Secur.* **10** 1–26
[40] Gomez S, Arenas A, Borgeholthoefer J, Meloni S and Moreno Y 2010 Discrete-time Markov chain approach to contact-based disease spreading in complex networks *Europhys. Lett.* **89** 275–88
[41] Fleming W H and Rishel R W 1975 *Deterministic and Stochastic Optimal Control* (New York: Springer)
[42] Kandhway K and Kuri J 2016 Optimal resource allocation over time and degree classes for maximizing information dissemination in social networks *IEEE/ACM Trans. Netw.* **24** 3204–17

J. Stat. Mech. (2018) 123402